High Sensitivity Handheld Analog Readout Circuit for Microfluidic Based Electrical Impedance Sensing

Niloy Talukder, Tuan Le, Pengfei Xie, Steve Orbine, Xinnan Cao, and Mehdi Javanmard
Department of Electrical and Computer Engineering
Rutgers, the State University of New Jersey
Piscataway 08854, United States
email: mehdi.javanmard@rutgers.edu, niloy.talukder@rutgers.edu

***Abstract*— In this paper, we present a novel lock-in-amplifier design analog readout of a microfluidic based impedance cytometer which is portable, low cost and capable of detecting 8 micron bead with a signal to noise ratio (SNR) of 184. Phase mismatch between sensor signal and the reference signal, which is a major concern in lock-in-amplifier design does not pose any problem in our detection technique. The circuit board was tested with gold electrodes micro-patterned on a glass substrate. This design can be further improved for submicron biological cell characterization and detection while we can miniaturize the circuit size and reduce cost significantly.**

Keywords—biochip; analog lock in amplifier; impedance cytometer; microfluidics.

I. INTRODUCTION

Flow cytometry, a gold standard technique for cell characterization, is based on optical detection of fluorescently labeled biological cells and particles and requires bulky and costly optical instrumentation and expensive labeling of biomolecules [1]. On the other hand, electrical detection is advantageous over other detection techniques in the sense that it enables cheaper, lightweight detection. Portable medical devices based on electrical detection are a major field of research now. The portable medical device industry is currently worth $7.8 billion, which is expected to cross $20 billion by 2018 [2].

Electrical detection of cells can be performed based on impedance spectroscopy (IS) which involves measuring the impedance of biological cells over a wide range of frequencies [3]. The focus of this paper is on improving the sensitivity of the analog-front-end circuitry of microfluidic based impedance cytometers, as they allow for single cell detection capability making it an ideal candidate for disease diagnosis. The impedance spectroscopy microfluidic cytometer is scalable and can be integrated into a PCB with a CMOS compatible readout circuit, which makes it a good candidate for designing portable medical devices [1].

One of the major challenges of electrical impedance detection is detecting low SNR output signals provided by low voltage low power sensors which can be orders of magnitude smaller than electrical noise and interference signals from environment. Lock-in-amplification (LIA) which uses synchronous phase sensitive detection (PSD) technique is very effective for detecting very small AC signals size going down to few nano-volts. A narrow bandwidth around the modulation frequency is allowed to pass through to the output and the remaining signal is filtered out. Thus a signal which is a thousand times weaker than the noise environment can be successfully detected [4]. Using a high frequency reference signal for IS shorts out capacitive coupling in the sensor, and the output signal can be linearly amplified and detected using LIA technique. Hywel Morgan et al. [5] pointed out that the upper frequency (like 500 kHz) is limited by sampling rate of data acquisition system which has to be more than twice according to nyquist rate. In LIA, a multiplier is used to demodulate the carrier frequency and the peak frequency to baseband and a low pass filter is used to detect low frequency sensor signal and filter out high frequency signal and noise. But overall dc offset due to carrier frequency amplitude and active circuit components hinders further amplification at the output of low pass filter by forcing the signal out of rail of the power supply with high gain. Marcellis et al. [6] reported fixed voltage gain of as high as 10^4.

Lock-in-amplifier can be analog or digital. Digital LIA has gained popularity as it is suitable for multi-frequency operation [5, 7], thus commercial lock-in-amplifiers often use digital architecture [8]. However, to develop a portable hand-held lock-in-amplifier where single frequency excitation is sufficient, the use of a digital architecture may be over-kill. Also, digitizing the analog output of the sensor, which is a small peak carried on a baseline signal which drifts randomly with time, requires a very high resolution and high-end analog-to-digital converter. As a result of rapid scaling in CMOS transistor size, analog design enables miniaturization and low cost design. A fully analog lock-in-amplifier is thus an appropriate solution for miniaturized integrated portable medical devices. In the literature various analog LIA chip architectures have been presented [6, 9-12] where the main trend is to move from double to single supply, decreasing supply voltage, decreasing power supply consumption,

reduction in chip area, and exploiting new architectures to improve performance.

In this paper, initial development of an electrical impedance biosensor readout circuit design is presented that exploits a novel idea of using a dc blocking capacitor for drift and carrier frequency component subtraction in analog domain, and post-subtraction amplification which results in enhanced sensitivity of the output signal. We achieved gain as high as 1.1 x 10^6. High gain also amplifies the noise level of the system, however the signal peak dominates over the noise. Phase mismatch in sensor signal and reference signal does not pose a problem for the detection technique. We discuss in detail the design methodology and circuit analysis of our analog readout circuit that we used for isolating the very weak signal generated by bead flow from the noisy environment in the sensor. The theoretical noise model is described and the noise simulation result is presented. Then the readout circuit is practically implemented on a printed circuit board and tested with a microfluidic based impedance cytometer which has gold electrodes micro-patterned on a glass substrate. The noise power spectral density of the circuit and biosensor under test is measured. A unique upward and downward peak signature corresponding to single beads helps to differentiate the true peak from the noise floor even with low signal to noise ratio. The output signal of readout circuit is de-noised, low pass filtered and further processed in MATLAB. Low manufacturing cost and portability make it suitable for point of care diagnosis in low resource settings, such as in developing countries [13].

II. LOCK-IN-AMPLIFIER BASED BIOSENSING TECHNIQUE

The lock-in-amplifier consists of a trans-impedance amplifier, a mixer, a low pass filter, a high pass filter, and high gain. Experiments show that for the frequency region between 100kHz and 1 MHz, impedance is dominated by bulk solution resistance across the electrolyte. Above 1 MHz frequency there is a drop in impedance [1]. We used an excitation frequency of 500 kHz. The modulated current signal peaks are converted into a voltage signal using a trans-impedance amplifier. Then a mixer stage demodulates the voltage signal by multiplying it with the input frequency. The demodulated signal is then passed through a low pass filter stage with low cut off frequency (100 Hz) so that only the signal peak of interest gets through it. In addition to the input frequency, high frequency noise components are filtered out which improves signal to noise ratio of our system. The low pass filter cut off frequency is determined based on the transit time of the bead between two electrodes. The output of the low pass filter is

$$V_{LPF} = \frac{1}{2} V_{TIA} V_{sig} [1 + mx(t)] \cos \Theta_{sig} \quad (1)$$

where, V_{TIA} and V_{sig} are the amplitudes of the output of the trans-impedance amplifier and the input reference signal respectively, $mx(t)$ is a time varying component, and Θ_{sig} is the phase of the input signal. So, the phase mismatch between input and output of the multiplier does not influence the system output. A blocking capacitor is used to remove the dc component so only $mx(t)$ component remains which is amplified using high gain stages. The concept of the lock-in-amplification based biosensor is illustrated in Fig. 1.

III. NOISE ANALYSIS FOR READOUT CIRCUIT

In this section, the calculation for output referred voltage noise and noise simulation result of our circuit is presented. Fig. 2 illustrates noise model of the circuit.

The calculation of the output referred voltage noise of the circuit is discussed here. The output voltage noise of the trans-impedance stage is:

$$E_{n1}{}^2 = \left(\frac{R_{f1}}{R_{biosensor}}\right)^2 \left(V_{biosensor}{}^2 + V_{n1}{}^2\right) + R_{f1}{}^2 i_{n1}{}^2 + V_{f1}{}^2 \quad (2)$$

The output voltage noise of the mixer stage is:

$$E_{n2}{}^2 = E_{n1}{}^2 + V_{mix}{}^2 \quad (3)$$

The output voltage noise of the active low pass filter stage is:

$$E_{n3}{}^2 = \left(\frac{Z_{c1}}{(R_1 + R_2||Z_{c2} + Z_{c1})}\right)^2 (E_{n2}{}^2 + V_1{}^2) + Z_{c1}{}^2 \left(\left(\frac{\begin{vmatrix} V_2 & -R_2 \\ -V_2 & R_2+Z_{c2} \end{vmatrix}}{\begin{vmatrix} R_1+R_2+Z_{c1} & -R_2 \\ -R_2 & R_2+Z_{c2} \end{vmatrix}} \right)^2 + \left(\frac{\begin{vmatrix} V_{n2} & -R_2 \\ -V_{n2} & R_2+Z_{c2} \end{vmatrix}}{\begin{vmatrix} R_1+R_2+Z_{c1} & -R_2 \\ -R_2 & R_2+Z_{c2} \end{vmatrix}} \right)^2 \right) + i_{n2}{}^2 \left[\frac{(R_1 + R_2||Z_{c2})Z_{c1}}{R_1 + R_2||Z_{c2} + Z_{c1}}\right]^2 + \left(V_{f2} + Z_{c1} \left(\frac{\begin{vmatrix} R_2+Z_{c2} & V_{f2} \\ -R_2 & 0 \end{vmatrix}}{\begin{vmatrix} R_2+Z_{c2} & -R_2 \\ -R_2 & R_1+R_2+Z_{c1} \end{vmatrix}} \right) \right)^2 \quad (4)$$

The output voltage noise of the cascaded passive low pass filter and DC blocking capacitor is:

$$E_{n4}{}^2 = \left(\frac{E_{n3} - V_3}{R_3 + Z_{c3}}\right)^2 Z_{c3}{}^2 \quad (5)$$

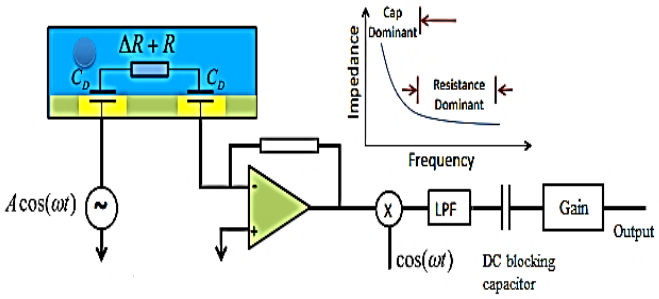

Fig. 1. Lock-in-amplifier based resistive biosensor.

The output voltage noise of Inverting Gain Stage 1 is:

$$E_{n5}{}^2 = \left(R_{f3}/R_4\right)^2\left(V_4{}^2 + V_{n3}{}^2 + E_{n4}{}^2\right) + R_{f3}{}^2 i_{n3}{}^2 + V_{f3}{}^2 \quad (6)$$

The output voltage noise of Inverting Gain Stage 2 is:

$$E_{n6}{}^2 = \left(R_{f4}/R_5\right)^2\left(V_5{}^2 + V_{n4}{}^2 + E_{n5}{}^2\right) + R_{f4}{}^2 i_{n4}{}^2 + V_{f4}{}^2 \quad (7)$$

Here, the variables are presented in Fig. 2. V_n and i_n correspond to input referred voltage and current noise of operational amplifier and they are numbered according to their order in circuit. Each resistor is also modeled as a thermal voltage source. Capacitors do not serve as independent noise sources.

The circuit was simulated using LTSpice IV simulation software. The simulation result closely matches with the theoretical calculation. The output voltage noise frequency spectrum simulation of the circuit in LTSpice is shown in Fig. 3. Inclusion of two high gain stages increases noise to 1.2 mV/√Hz within the period of frequency 10 Hz and 100 Hz. The total estimated RMS noise value from the simulation is 26.127 mV.

IV. BIOSENSOR FABRICATION

The microfluidic device is fabricated using standard photolithography [14]. The microfluidic channel is constructed by casting polydimethylsiloxance (PDMS) on the master mold. The master mold is fabricated on the Si wafer by micro-patterning and exposing to UV light SU-8 photoresist. In our design, the channel is 300 µm wide, 8 µm high, and 1 cm long. PDMS solution is degassed in a vacuum desiccator and poured slowly onto the mold in a container. The PDMS solution is cured for 1 hour in 80°C before peeling it off from the master mold.

The microfluidic biosensor is fabricated with gold electrodes on a glass wafer using standard photolithography, electron beam evaporation, and a lift-off process. The glass wafer is spin-coated with AZ5214 photoresist before micro-patterning the electrode configuration and exposing to UV

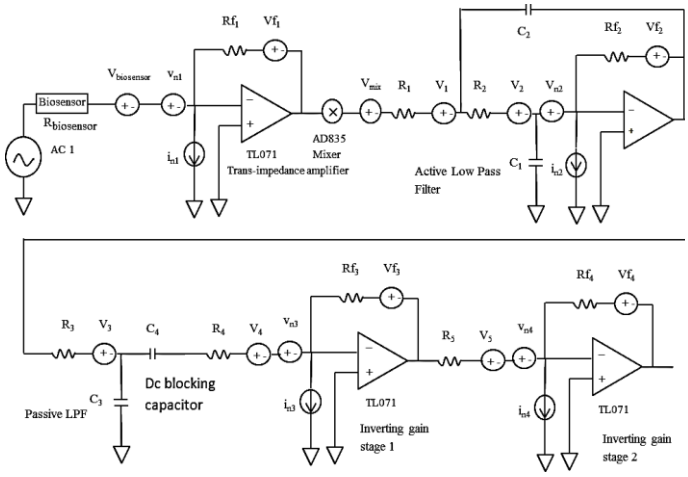

Fig. 2. Noise model of the analog readout circuit

light. The electron beam evaporation process deposits a layer of chromium (50 Angstrom) and a layer of gold (100 nm) to the glass substrate. In the design, the electrodes are 10 µm wide and 15 µm apart from each other.

PDMS is exposed to oxygen plasma generating a thin layer of silanol (SiOH) terminations, which form the conformal bonding to the oxidized surface of the glass wafer [15]. The microfluidic channel is aligned perpendicular to the the electrode fingers. Oxygen plasma treatment on PDMS changes its surface properties from hydrophobic to hydrophilic [16]. Intrinsically, PDMS is hydrophobic, making it difficult to wet the micro channel. A schematic of biosensor is shown in Fig. 4.

V. CIRCUIT DESCRIPTION AND EXPERIMENTAL SETUP

The block diagram of the experimental setup is shown in figure 5. Two EBL 6F22 9V 600 mAh lithium ion rechargeable batteries are used as the power supply. There is a DPDT toggle switch to turn on and off the batteries. The batteries can supply power for approximately 12 hours. Two

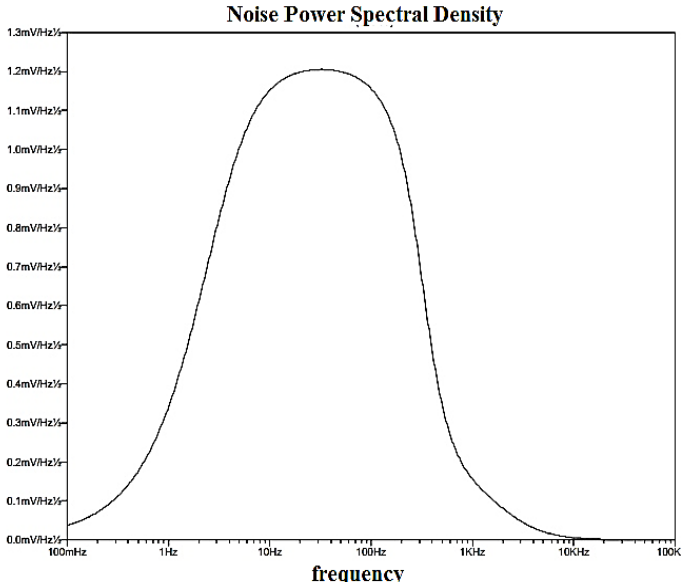

Fig. 3. Noise simulation of the readout circuit

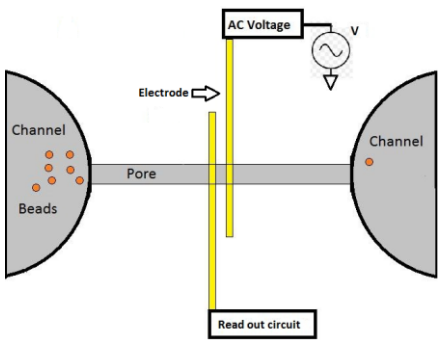

Fig. 4. Schematic of the biosensor and connection to the circuit

voltage regulators (LT1763 and LT1964 from Linear Technology) are used to get +5V and -5V respectively from 9V batteries. On the circuit board, we have considered the power supply bypassing technique for both high and low frequency noise rejection. Two electrode pads from the biochip are connected to the readout circuit through clips. A relatively high frequency (500 kHz) $2V_{p-p}$ input signal is generated on board from a 1 MHz crystal oscillator ECS-100AC and a passive LC tank and then fed into the biosensor. The higher the amplitude of input signal, the higher will be the SNR. We considered $2V_{p-p}$ signal so that dc offset of the subsequent stages do not bring signal to rail and clip it. The input signal has a resolution of 20 mV and the spectrum of the bandpass passive LC filter tank is shown in Fig. 6. The center of the band is at 500 kHz so it rejects all other frequencies and gives a smooth sine wave signal. The AC signal goes into the biochip through one electrode pad and the output current from biochip is collected through the other electrode pad. To implement the trans-impedance stage, a low noise operational amplifier (TL071CP from Texas Instruments) has been used. In the feedback path a 20 kΩ potentiometer is used alongside a 2 kΩ resistor to control the trans-impedance gain. So, the trans-impedance gain is between 0.04 to 0.44. The mixer stage is implemented using a four quadrant multiplier (AD835

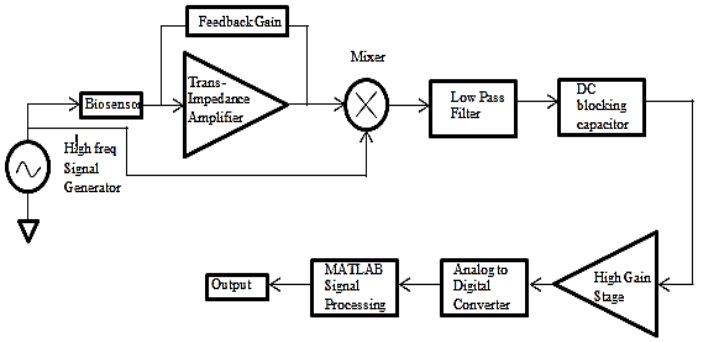

Fig. 5. System block diagram.

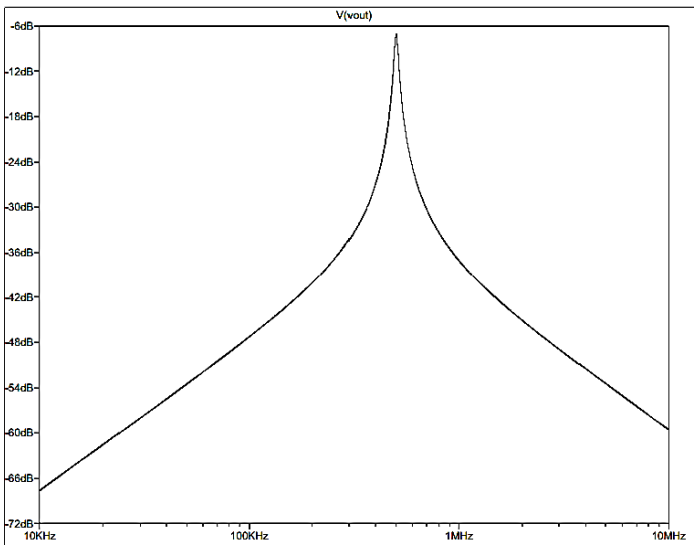

Fig. 6. Gain versus frequency plot for passive LC tank. Center of band is at 500 kHz.

from Analog Devices). A 3rd order butterworth low pass filter (cut off 100 Hz) is implemented using the same low noise operational amplifier TL071CP. This filter gives 60 dB roll off per decade and rejects high frequency noise. We have used a DC blocking capacitor. At the final stage of the circuit, two inverting high gain stages are used to amplify the detected peak from the biosensor. The first inverting stage has a gain of 1000. The second inverting stage has a potentiometer for adjustable gain between 100 and 1100. So, we can achieve a gain as high as 1.1MΩ. The potentiometer was set to minimum during the experiment so the net gain was 10^5. In the PCB we used a two layer ground plane to reduce crosstalk between wires and made sure there was no potential difference between the ground connection of the different circuit elements [17]. The dimensions of our printed circuit board was 100 mm x 80 mm and the total cost of manufacturing PCB and the circuit components was around $70. A BNC cable was used to collect the output signal of the readout circuit. The analog output of the readout circuit was converted to digital signal using (National Instruments RIO USB 7856R) a multipurpose data acquisition card. The output voltage signal was reconstructed and post-processed using Labview software. The recorded data was processed in MATLAB 2012a (Mathworks Inc.). An image of PCB and biosensor is illustrated in figure 7.

VI. NOISE POWER SPECTRAL DENSITY OF LOCK-IN-AMPLIFIER

We have measured the noise power spectral density by grounding the input of our circuit. We have measured the noise level of the circuit for the following five cases:

1) The PCB with no biosensor connected.

2) The PCB connected to the biosensor but no fluid in it.

3) The PCB with 50 kΩ resistor in place of the biosensor

4) The PCB and the biosensor with fluid and beads in it.

5) The DAQ card input shorted to measure its noise.

The results are overlaid in Fig. 8. From the figure it is seen that noise from the first four cases dominate over the DAQ

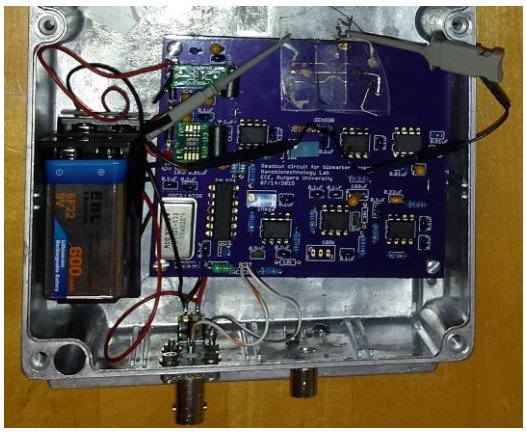

Fig. 7. Printed circuit board with biochip

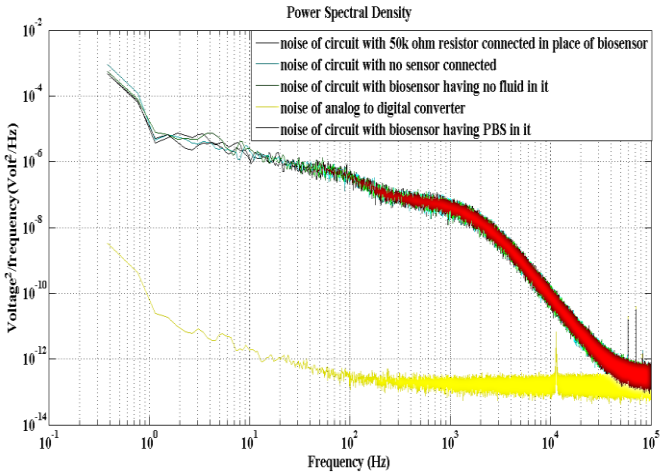

Fig. 8. The noise power spectral density for various components of the system.

card noise. The low frequency flicker noise comes from the DAQ card and contributes to the PCB noise. The PCB noise with the 50 kΩ resistor is similar to noise of PCB with biosensor so a 50 kΩ resistor is used in the noise simulation in place of the biosensor. The total estimated RMS noise value from the PCB and biosensor with fluid and beads in it is 73.47 mV. This noise is nearly 3 times of that obtained in simulation. During simulation, the +5V, -5V regulator circuit and on board frequency generator circuit is not considered, which contributes to extra noise. Also interference noise from environment adds more noise. Low frequency flicker noise from the circuit active elements and also from the measuring DAQ system, which is absent in simulation, further increases experimentally observed noise. The simulation models that we have used for the opamp also cannot simulate the flicker noise. Even when the noise measurement was done in the metal box there was no significant noise reduction in the measurement. Also during experiment it was necessary to observe the channel under microscope to monitor bead flow, so we could not cover the metal box.

VII. EXPERIMENT

In the experiment, 8 micron beads were used in the biosensor to test functionality of the readout circuit. After doing oxygen plasma etching on the biosensor for getting bead flow, phosphate-buffered saline (PBS) is poured onto the channel pore and then beads are dropped in the channel using micropipette. Using hydraulic pump 11 eilte diffusion only dual syringe (model number 704501 from Harvard Apparatus), a steady flow of 0.08 µl/min was set in the sensor. The signal coming out of PCB was recorded in Labview software using an NI DAQ system. Transit time for bead to pass by the distance between two electrodes was between 0.13 to 0.15 sec. So, signal peaks had frequency in between 6 to 8 Hz and with low pass filter cutoff of 100 Hz the signal peaks could easily get through. The current that was recorded from the sensor was around 20 nA. Channel under optical microscope was simultaneously monitored to confirm that electrical signal changes were due to beads passing through the electrodes. Video recordings of the passage of beads through the channel were acquired to confirm that each peak indeed corresponded to passage of beads through the electrode finger. An image that shows different stages of single bead flow through channel pore is presented in Fig. 9.

VIII. RESULT ANALYSIS

In MATLAB, a Chebyshev low pass filter and wavelet de-noising technique to lower noise was used to get smooth peaks. The sample output signal corresponding to an 8 micron bead is shown in Fig. 10.

The output signal of the low-pass filter stage is a sharp positive peak with a baseline that drifts over time. The DC blocking capacitor removes the baseline however adds a negative overshoot. This small negative overshoot is greatly amplified by two high gain stages and ends up as a signature

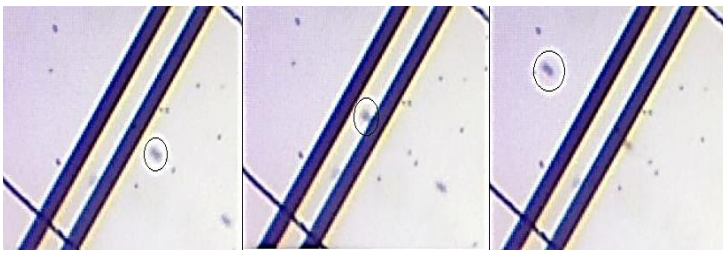

Fig. 9. 8 micron bead flowing through 2 electrode sensor.

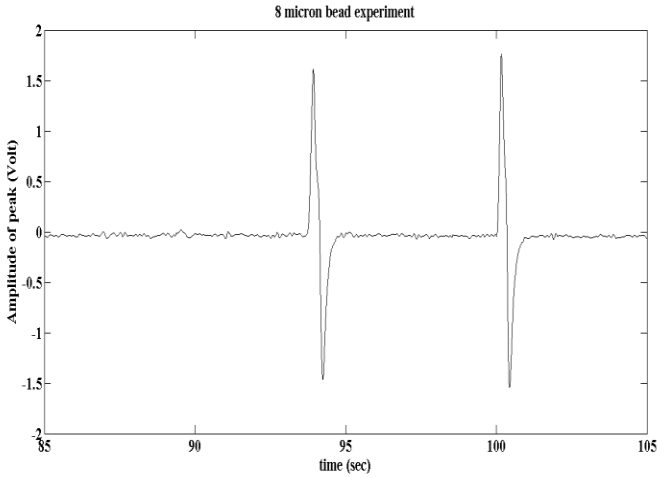

Fig. 10. Recorded signal after MATLAB signal processing

Bead	Signal to Noise Ratio (SNR)		Percentage of Bead Volume with Respect to Active Sensing Channel Volume
	Raw	Processed	
8 micron	40	184	0.55%

Table 1. SNR and percentage of bead volume with respect to active sensing channel volume for 8 micron bead flow.

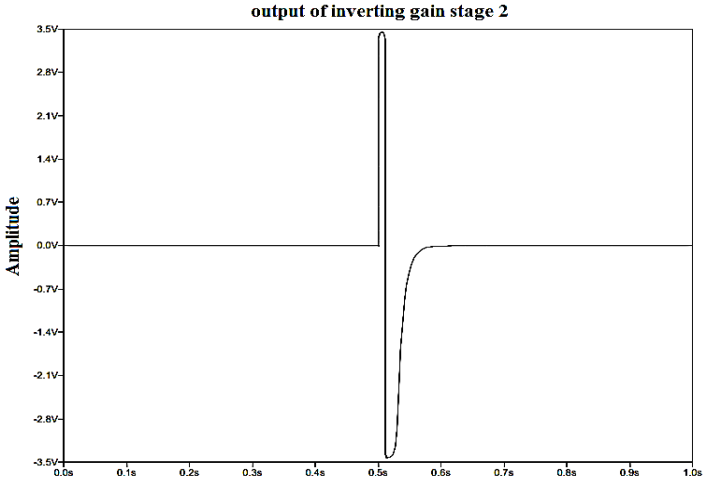

Fig. 11. Simulation result to justify the nature of the peak by showing output of the second Inverting Gain Stage.

positive then negative peak at the output of the circuit. The phenomenon was verified using LTSpice IV simulation software. In Fig. 11, the simulated output of the second inverting gain stage is presented.

IX. CONCLUSION AND FUTURE WORK

Here, a novel lock-in-amplifier design is presented to implement the analog readout circuit for a microfluidic based impedance cytometer capable of detecting 8 µm beads with a signal to noise ratio (SNR) of 184. The circuit can detect beads which have volumes only 0.55% of the total active sensing volume. Future work will focus on developing a fully integrated CMOS solution for further improving the detection limit, reducing the overall size and power consumption of the system and also providing wireless connectivity.

ACKNOWLEDGMENT

The authors would like to thank Professor M. Caggiano from Electrical and Computer Engineering Department, Rutgers University for useful discussions, and Zhongtian Lin and Azam Gholizadeh from the Nanobiotechnology Laboratory of Rutgers University for help with sensor fabrication.

REFERENCES

[1] S. Emaminejad, K H Paik, V. T. Cossa, and M. Javanmard, "Portable Cytometry Using Microscale Electronic Sensing." *Sensors and Actuators B: Chemical* (2015).

[2] "Portable Medical Devices Market Worth $20 billion by 2018" [online] Available: 2013, http://www.marketsandmarkets.com/ PressReleases/semiconductor-opportunities-mobile-healthcare.asp (Accessed: 28th November, 2015).

[3] H.E. Ayliffe, A. B. Frazier, and R.D. Rabbitt, "Electric impedance spectroscopy using microchannels with integrated metal electrodes", Journal of Microelectromechanical Systems, Vol. 8 , Issue 1 , pp. 50-57 (1999).

[4] About Lock-In Amplifiers, Application Note #3, Stanford Research Systems, [online] Available: 1999, http://www.thinksrs.com /downloads/PDFs/ ApplicationNotes/AboutLIAs.pdf (Accessed: 28th November, 2015).

[5] T. Sun, D. Holmes, S. Gawad, N. G. Green, and H. Morgan, "High speed multi-frequency impedance analysis of single particles in a microfluidic cytometer using maximum length sequences," *Lab on a chip* 7, no. 8 pp. 1034-1040, 2007.

[6] A. D. Marcellis, G. Ferri, P. Mantenuto, and D'Amico, "A new single-chip analog lock-in amplifier with automatic phase and frequency tuning for physical/chemical noisy phenomena detection," In Proceedings of the IEEE Workshop on Advances in Sensors and Interfaces (IWASI), pp. 121–124, Bari, Italy, 13–14 June 2013.

[7] C. Yang, S. R. Jadhav, R. M Worden, and A. J. Mason. "Compact low-power impedance-to-digital converter for sensor array microsystems." *Solid-State Circuits, IEEE Journal of* 44, no. 10 pp. 2844-2855, 2009.

[8] HF2IS Impedance Spectroscope, Zurich Instruments, [online] Available: https://www.zhinst.com/products/hf2is (Accessed: 28th November, 2015)

[9] KH Lee, et al. "A CMOS impedance cytometer for 3D flowing single-cell real-time analysis with ΔΣ error correction," Solid-State Circuits Conference Digest of Technical Papers (ISSCC), IEEE International, 2012, pp. 304-306.

[10] A. Manickam, CA Johnson, S. Kavusi, and A. Hassibi, "Interface design for CMOS-integrated electrochemical impedance spectroscopy (EIS) biosensors," Sensors vol. 12, (11), pp. 14467-14488, 2012.

[11] P. Kassanos, L. Constantinou, IF Triantis, and A. Demosthenous, "An Integrated Analog Readout for Multi-Frequency Bioimpedance Measurements," Sensors Journal, IEEE vol. 14, (8), pp. 2792-2800, 2014.

[12] J. Gu, and N. McFarlane. "A low power multi-frequency current mode lock-in amplifier for impedance sensing." In *Instrumentation and Measurement Technology Conference (I2MTC), 2015 IEEE International*, pp. 494-499. IEEE, 2015.

[13] S. Emaminejad, M. Javanmard, R. W. Dutton, and R. W. Davis, "Microfluidic diagnostic tool for the developing world: Contactless impedance flow cytometry," Lab on a Chip, vol. 12(21), pp. 4499-4507, 2012.

[14] Y. Xia, and G. M. Whitesides. "Soft lithography." *Annual review of materials science* 28, no. 1 (1998): 153-184.

[15] D. C. Duffy, J. C. McDonald, O. JA Schueller, and George M. Whitesides. "Rapid prototyping of microfluidic systems in poly (dimethylsiloxane)." *Analytical chemistry* 70, no. 23, pp. 4974-4984, 1999.

[16] S. H. Tan, N. T. Nguyen, Y. C. Chua, and T. G. Kang. "Oxygen plasma treatment for reducing hydrophobicity of a sealed polydimethylsiloxane microchannel," *Biomicrofluidics* 4, no. 3 032204, 2010.

[17] PCB Design Guidelines for reduced EMI Texas Instruments [online] Available: 1999, http://www.ti.com/lit/an/szza009/szza009.pdf (Accessed: 28th November, 2015)